

SCIENTIFIC REPORTS

OPEN

Bacterial inactivation by plasma treated water enhanced by reactive nitrogen species

Priyanka Shaw^{1,2}, Naresh Kumar^{1,2}, Hyong Sin Kwak¹, Ji Hoon Park¹, Han Sup Uhm¹, Annemie Bogaerts², Eun Ha Choi¹ & Pankaj Attri^{1,2}

There is a growing body of literature that recognizes the importance of plasma treated water (PTW) for inactivation of microorganism. However, very little attention has been paid to the role of reactive nitrogen species (RNS) in deactivation of bacteria. The aim of this study is to explore the role of RNS in bacterial killing, and to develop a plasma system with increased sterilization efficiency. To increase the concentration of reactive oxygen and nitrogen species (RONS) in solution, we have used vapor systems (DI water/HNO₃ at different wt%) combined with plasma using N₂ as working gas. The results show that the addition of the vapor system yields higher RONS contents. Furthermore, PTW produced by N₂ + 0.5 wt% HNO₃ vapor comprises a large amount of both RNS and ROS, while PTW created by N₂ + H₂O vapor consists of a large amount of ROS, but much less RNS. Interestingly, we observed more deactivation of *E. Coli* with PTW created by N₂ + 0.5 wt% HNO₃ vapor plasma as compared to PTW generated by the other plasma systems. This work provides new insight into the role of RNS along with ROS for deactivation of bacteria.

Over the last decade, several novel techniques have been developed for microbial decontamination^{1,2}. Atmospheric pressure non-thermal plasma (NTP) has emerged as a potential tool for the effective control of photogenic microorganisms, and for water purification^{3,4}. NTP generates ions, ozone (O₃), UV photons, and various reactive oxygen and nitrogen species (RONS)^{5,6}. It has shown promising effect in the sterilization of medical tools and packaging materials⁷. Recently, NTP has also shown its efficiency in wound healing⁸⁻¹¹, tissue regeneration^{12,13} and cancer therapy¹⁴⁻¹⁷. Many types of plasma devices have been developed, such as dielectric barrier discharges (DBDs), plasma jets, floating electrode (FE)-DBD, and external additives have also been combined to the plasma treatment in order to increase the efficiency¹⁴⁻¹⁶. Previously, we have investigated the influence of H₂O and D₂O vapor to increase the efficiency of an atmospheric pressure plasma jet (APPJ) for the inactivation of cancer cells, i.e., breast cancer and melanocytes cancer cells^{14,16}. In the last few years, plasma treated physiological fluids have also shown promising effect, similar to the direct treatment of plasma¹⁷⁻¹⁹. These plasma treated solutions contain reactive species with a longer lifetime, and provide a medium with a high and durable degree of reactivity²⁰.

The chemical species generated in liquid treated by plasma mainly depend upon the type of discharge, feeding gas, humidity, etc. It was stated that plasma treated water (PTW) consists of various RONS, such as O (atomic oxygen), OH (hydroxyl radicals), O₃ (ozone), H₂O₂ (hydrogen peroxide), NO (nitric oxide), NO₂⁻ (nitrites), NO₃⁻ (nitrates) and ONOO⁻ (peroxynitrites) that are responsible for microbial inhibition²¹. However, other authors conclude that short lived species are not stable in PTW, i.e., the life-time of excited atomic oxygen is ≈30 ns²², for OH it is ≈1 ns²³, while O₃ can live for 1000 s at room temperature²⁴. It was also reported that reactive oxygen species (ROS), e.g. OH, O₂^{•-}, O₃ and H₂O₂, play a significant role in bacterial inactivation^{25,26}, whereas other research groups proposed that ONOO⁻ is the dominant species for bacterial inactivation^{27,28}. Furthermore, it was reported in literature that the presence of NO₂⁻/NO₃⁻ at acidic pH in noticeable concentrations can cause the antimicrobial properties^{29,30}. Traylor *et al.* discussed the complexity of reactions in PTW with biological systems, because different biological effects occur in differing time scales with various chemical components²⁵. Finally,

¹Plasma Bioscience Research Center, Department of Electrical and Biological Physics, Kwangwoon University, 20 Kwangwon-Ro, Nowon-Gu, Seoul, 139-701, Korea. ²Research group PLASMANT, Department of Chemistry, University of Antwerp, BE-2610, Wilrijk-Antwerp, Belgium. Priyanka Shaw and Naresh Kumar contributed equally to this work. Correspondence and requests for materials should be addressed to E.H.C. (email: ehchoi@kw.ac.kr) or P.A. (email: chem.pankaj@gmail.com)

Ikawa *et al.* suggested that the main component for the antibacterial activity of PTW is not ONOOH (peroxynitrous acid), but O_2NOOH (peroxynitric acid)³¹.

In general there is still uncertainty whether ROS or RNS are the main factor for the antibacterial effect in PTW. This paper aims to provide an answer to this research question about the importance of ROS and/or RNS in PTW for the antibacterial efficacy. Therefore, we developed an APPJ system with HNO_3 vapor at different wt% and we checked the enhancement of NO along with OH radicals, both in the gas and liquid phase, using optical emission spectroscopy and chemical analysis, respectively. Besides NO and OH, the production of other reactive species, such as H_2O_2 , NO_2^- and NO_3^- , was also detected in solution after different types of plasma treatment (i.e., only N_2 gas plasma, $N_2 + H_2O$ vapor plasma, and $N_2 + 0.5$ wt% HNO_3 vapor plasma). Subsequently, we compared the antibacterial activity of PTW generated by the different plasma systems, by treating *E. coli*. Finally, we measured the oxidative stress related gene expression using quantitative real time polymerase chain reaction (qPCR) analysis, the genomic DNA degradation using gel electrophoresis, and changes in the surface morphology using scanning electron microscopy (SEM) of *E. coli* after treatment with PTW.

Experimental Section

Chemicals. Luria Bertani agar and broth were purchased from MB cells (Seoul, Korea). Strains of *Escherichia coli* (11775) were procured from the American Type Culture Collection, USA (ATCC). Penicillin–streptomycin was purchased from Gibco BRL (Carlsbad, CA, USA). Terephthalic acid and sodium hydroxide were purchased from Sigma Aldrich. Genomic DNA extraction and RNA extraction were done through a DNA extraction kit (GeneAll, Exgene Cell SV MAXI, Banseok Bld, Seoul, Korea) and a RNA extraction kit (RNeasy Mini Kit, Qiagen). cDNA synthesis was performed using the ReverTra Ace qPCR RT Master Mix with gDNA Remover kit (Toyobo, Japan), and quantitative PCR was performed using a Thunderbird Sybr[®] qPCR Mix kit (Toyobo, Japan).

Plasma device and characterizations. The APPJ that was used consists of a needle-type powered (stainless steel) electrode that is enclosed by a quartz tube with inner diameter of 3 mm, outer diameter of 5 mm, and length of 9 mm. We used different flow rates of N_2 gas in combination with different flow rates of H_2O/HNO_3 solution, so that the final gas flow rate remains 1000 cubic centimeters per minute (ccm). We applied an input voltage of 70 V, yielding an electrical power of about 7 W (2.2 kV, 11 mA with phase angle of 60° between current and voltage). The N_2 gas flow rate directly introduced into the plasma was varied between 200 and 1000 ccm. Accordingly, the amount of N_2 flowing through the solution of DI water with 0.5, 1 or 3 wt% HNO_3 , to generate H_2O/HNO_3 vapor that was fed into the plasma, also varied from 200 to 800 ccm. The combined gas (i.e., gas with vapor or without vapor) was injected into the needle of the plasma jet, and was flowing out through a 1 mm hole, as shown in Fig. 1a. Spectra of the APPJ emission were recorded by HR4000CG-UV-NIR (Ocean Optics, FL, USA) over a wide wavelength range (200–1100 nm), for a humidity of 40%. The electron temperature was measured from the emission spectrum using the SPEAC air program.

Physical and chemical characterization of plasma treated water (PTW). After exposing the water samples for 10 min to either N_2 , $N_2 + H_2O$ vapor or $N_2 + HNO_3$ vapor plasma (at different wt% of HNO_3 , i.e., 0.5, 1 and 3 wt%), the pH and temperature of the sample were measured by a pH meter (Eutech Instruments, Singapore) and an Infrared (IR) camera (Fluke Ti100 Series Thermal Imaging Cameras, UK). Simultaneously, the RONS contents in the water samples were also analyzed. The amounts of OH and H_2O_2 were measured by previously described methods^{32,33}. The concentration of NO_2^- was measured using the Griess reagent kit (Molecular probe, USA) and the NO_3^- concentration was measured with an Acorn ion Meter (Oakton WD-WD-35613-30 Ion 6 meter).

To prepare the PTW, 2 ml of DI water was treated with plasma for 10 min in a 12-well plate, keeping 5 mm distance between the nozzle of the plasma jet device and the liquid surface. To determine the colony forming unit, gene expression, cell morphology and DNA damage, we used 1 ml PTW generated by the different plasma conditions, i.e., N_2 , $N_2 + H_2O$ vapor, and $N_2 + 0.5$ wt% HNO_3 vapor. The reason why we used the 0.5 wt% HNO_3 vapor in our further experiments on the antibacterial efficacy (instead of 1 and 3 wt%) is explained below.

Colony forming unit and disc diffusion assay. Strains of *Escherichia coli* (*E. coli*) were cultured in Luria broth (LB) media, until they reached the logarithmic growth phase of approximately 10^8 colony forming unit (CFU)/ml. To determine the CFU, the culture was incubated for 12 h at 37 °C, and shaken at 200 rpm. Aliquots of the culture (100 μ l) were pelleted by centrifugation at 5000 rpm for 5 min. The pellet was resuspended in 1 ml of PTW prepared by N_2 , $N_2 + H_2O$ vapor, and $N_2 + 0.5$ wt% HNO_3 vapor plasma, to determine the antimicrobial effects. The suspension was incubated for 3 h at room temperature, and shaken at 200 rpm. We also performed direct plasma treatment, for which we took the same growth phase of *E. coli* in 1 ml of water, and directly exposed it for 10 min with either N_2 , $N_2 + H_2O$ vapor, or $N_2 + 0.5$ wt% HNO_3 vapor plasma. Both the indirect and direct plasma treated samples were subjected to serial dilutions of 10^7 , 10^6 , 10^5 , 10^4 , and 10^3 CFU/ml. The samples were thoroughly mixed, and a tenfold serial dilution of each sample was transferred and spread uniformly on LB agar culture medium in a standard Petri dish (90 mm). The samples were then sealed and incubated at 37 °C for about 12 h, to count the CFUs. We measured a relative reduction compared to the control sample (for which the CFU was defined as 1 to evaluate the inactivation efficacy).

In addition, we performed another experiment on Disc diffusion to assess the antibacterial activity of the PTW, for which the antimicrobial susceptibility testing was carried out according to the standard method by Bauer *et al.*³⁴. The *E. coli* culture was evenly applied to LB agar culture plates using a sterile swab. The plates were dried for 15 min, and subsequently used for the sensitivity test. The discs that were impregnated with PTW produced by N_2 , $N_2 + H_2O$ and $N_2 + 0.5$ wt% HNO_3 vapor were placed on the LB agar surface. One positive control,

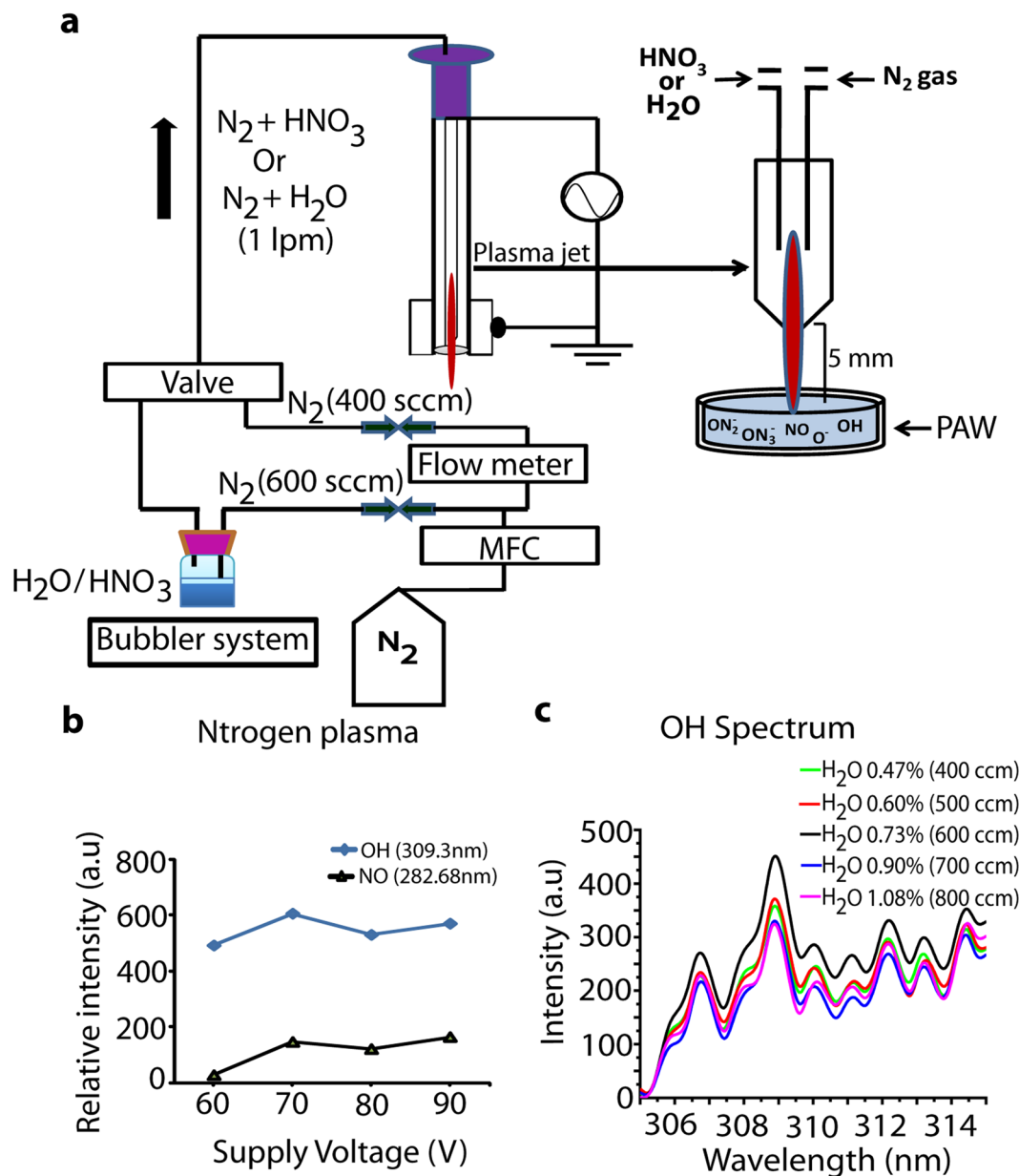


Figure 1. (a) Plasma setup; (b) Intensity of NO and OH spectral lines as a function of supply voltage in N_2 plasma; (c) OH spectra for different gas flow rates.

which was a disc, contained 30 μ g of standard commercial antibiotic (Penicillin). The plate was then incubated at 37 $^{\circ}$ C for 18 to 24 hours. After incubation, the plates were examined for the inhibition zone.

***E. coli* morphological analysis.** Scanning electron microscopy (SEM) (JSM 7001 F, JEOL, Tokyo, Japan) was applied to examine the morphology of the *E. coli* cells. Briefly, the bacterial samples exposed to PTW generated by either N_2 , $N_2 + H_2O$ vapor, or $N_2 + 0.5$ wt% HNO_3 vapor were fixed in 1 mL of Karnovsky's fixative (2% paraformaldehyde and 2% glutaraldehyde) overnight, as described in previous work⁵. The SEM sample preparation involved dehydration of the material in hexamethyldisilazane (HMDS), followed by mounting and coating on glass with carbon tape, and examination via SEM.

RNA extraction for quantitative real time PCR. To perform a quantitative evaluation of oxidative related gene expression, after 3 h exposure with PTW produced by N_2 , $N_2 + H_2O$ and $N_2 + 0.5$ wt% HNO_3 , the total RNA was extracted from treated and untreated samples of *E. coli* using an RNeasy Mini Kit, and it was converted to cDNA using reverse transcriptase and random primers (GoScriptTM Reverse Transcription System, Promega). The same amount of total RNA was used for the cDNA synthesis (Take3, Biotek). The resulting cDNA was used for the qPCR analysis (CFX96, Biorad) with primers (Macrogen) of 16s rRNA (the RNA component of the small subunit used as house-keeping gene), OxyR, RpoE, GroES, and DnaK.

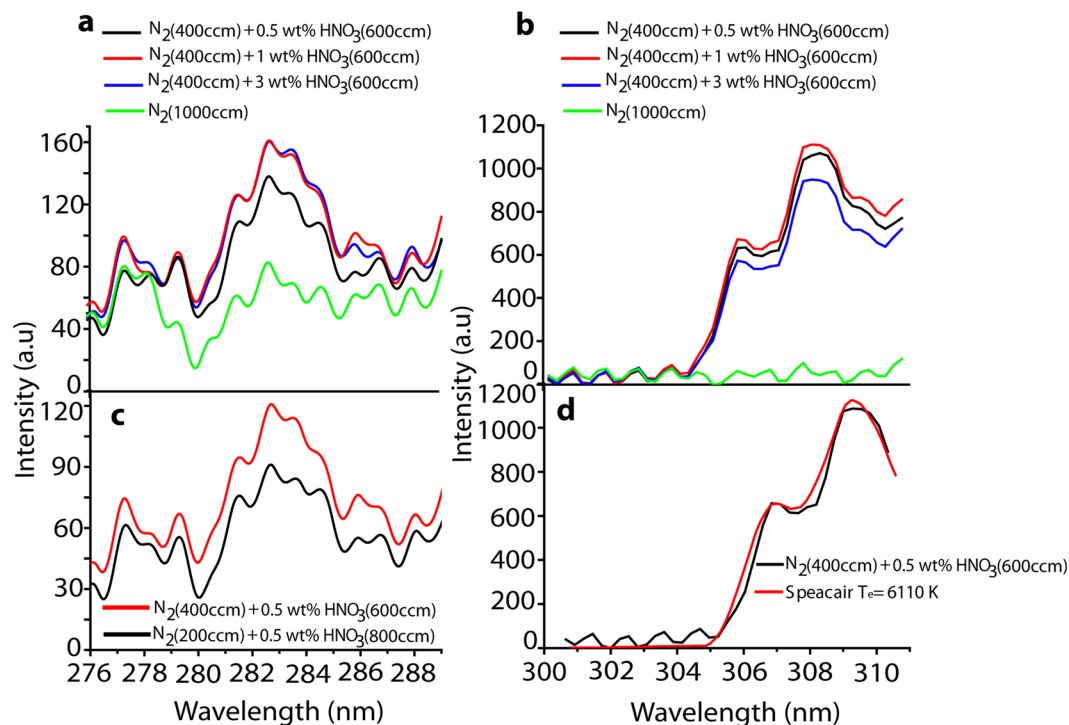


Figure 2. (a) NO spectra at different wt% of HNO₃ vapor plasma, (b) OH spectra at different wt% of HNO₃ vapor plasma, (c) NO spectra at different flow rates of N₂ gas, (d) Determination of the electron temperature using speacair for the OH spectrum.

The primer sequences used for the oxidative related mRNA expression in *E. coli* were:

Genes	Forward primers [5-3]	Reverse primers [5-3]
16S rRNA	AGAGCAAGCGACCTCATAA	TTCATGGAGTCGAGTTGCAG
OxyR	GGGAAACTGCTGATGCTG	CGCGGAAGTGTGTATCTTCA
RpoE	AGTCCCTCCCGGAAGATTTA	ACCTACCGGACAATCCATCCATGA
GroES	TGGCCGTATCCTTGAAAATG	CCGTAGCCATCGTTGAAAAT
DnaK	GAAGAAGCAGGCGACAAACT	TAGCGGCCTTTGTCTTCACT

DNA extraction for agarose gel electrophoresis. Genomic DNA was extracted after 3 h exposure with PTW produced by N₂, N₂ + H₂O and N₂ + 0.5 wt% HNO₃ for 1% agarose analysis. The treated cells were subjected to a genomic DNA extraction kit. Genomic DNA was extracted following a standard molecular biology protocol, and re-suspended in 50 µl water. The same amount of genomic DNA (2 mg) extracted from *E. coli* was loaded on a 1% agarose gel, and run for 1 h. After staining with ethidium bromide, the DNA bands were photographed.

Statistical analysis. All values are represented as the mean ± SD of the indicated number of replicates. Statistical analysis of the data was performed using the Student's t-test to establish the significance between the data points, and significant differences are based on *P < 0.05 or **P < 0.01.

Results

Determination of NO and OH intensities at H₂O vapor plasma condition. Figure 1(b) shows the NO and OH relative intensities during the plasma discharge, as a function of the applied voltage. Applying 70 V input voltage shows the high intensity of both NO and OH peaks measured through optical emission spectroscopy. Therefore, our further experiments were performed at an input voltage of 70 V. In order to evaluate the highest generation of OH radicals, we applied different flow rates of N₂ gas in H₂O solution, i.e., 400, 500, 600, 700, and 800 ccm, to generate the H₂O vapor along with the N₂ gas, and we examined the emission spectra of the plasma. Figure 1(c) shows that the OH emission peak was highest at 600 ccm of N₂ gas flow.

Determination of NO and OH intensities at HNO₃ vapor plasma conditions. We applied different wt% HNO₃ (0.5, 1 and 3 wt%) with a fixed N₂ gas flow rate, and we also compared with no HNO₃ vapor. Figure 2(a) shows that 1 and 3 wt% of HNO₃ vapor yields a high spectral intensity for NO, whereas Fig. 2(b) shows

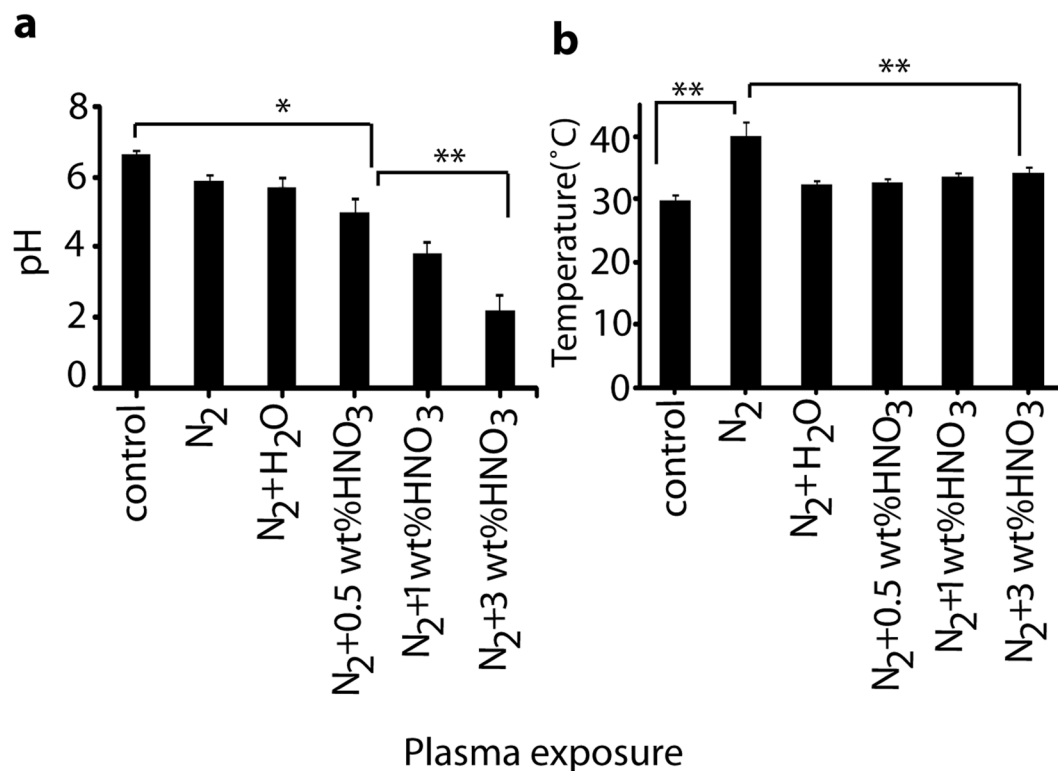


Figure 3. (a) pH and (b) temperature in DI water after exposure with plasma jet for 10 min, at different conditions: 1000 ccm N₂ plasma, or 400 ccm N₂ plasma with either H₂O or HNO₃ vapor at three different wt%, and comparison with untreated water sample (control).

that 0.5 wt% of HNO₃ vapor yields a high OH intensity. The further experiments are performed using 0.5 wt% HNO₃ vapor plasma, based on the change in pH of the solution after treatment (as described below).

We also analyzed the NO spectra for different flow rates of N₂ + 0.5 wt% HNO₃ vapor plasma. Figure 2(c) shows that N₂ with 600 ccm added to 0.5 wt% HNO₃ solution vapor, combined with 400 ccm of N₂ gas, resulted in a higher NO intensity, in comparison with 800 ccm N₂ added to 0.5 wt% HNO₃ solution vapor, combined with 200 ccm of N₂ gas. Finally, the electronic temperature in the plasma generated at N₂ (400 ccm) + 0.5 wt% HNO₃ vapor (with 600 ccm N₂ gas) was determined to be 6110 K using Specair, as shown in Fig. 2(d).

Determination of pH and temperature after plasma exposure. To determine the change in properties of PTW after exposure with plasma, we checked the pH and temperature for different conditions, i.e., N₂ (400 ccm) + (0.5, 1 or 3 wt%) HNO₃ vapor (in 600 ccm N₂ gas) plasma, N₂ (400 ccm) + H₂O vapor (in 600 ccm N₂ gas) plasma, and N₂ (1000 ccm) plasma without vapor. Figure 3(a) shows that 10 min treatment with plasma of N₂ (400 ccm) + (0.5, 1 and 3 wt%) HNO₃ vapor (in 600 ccm N₂ gas) drastically decreases the pH, as compared with N₂ + H₂O vapor plasma and N₂ plasma without vapor. On the other hand, there is only a slight rise in temperature (few °C) of PTW for N₂ (400 ccm) + (0.5, 1 and 3 wt%) HNO₃ or H₂O vapor (in 600 ccm N₂ gas) plasma, while there is a significant rise of about 10 °C for the N₂ plasma without vapor, as shown in Fig. 3(b).

Estimation of RONS contents in plasma treated water. We have also measured the concentration of various RONS generated in the solutions after exposure to plasma at different conditions, i.e., N₂ (400 ccm) + (0.5, 1 and 3 wt%) HNO₃ or DI water vapor (in 600 ccm N₂ gas), and 1000 ccm N₂ gas without vapor. Figure 4(a) shows that 10 min treatment by N₂ + H₂O vapor plasma yields a higher amount of OH species in the solution, compared with N₂ + (0.5, 1, and 3 wt%) HNO₃ vapor plasma, and especially compared with the pure N₂ plasma. The OH radicals are the main source of H₂O₂, and Fig. 4(b) indeed illustrates that the N₂ + H₂O vapor plasma produced the highest concentration (0.9 mM) of H₂O₂, while the N₂ + HNO₃ (0.5, 1, and 3 wt%) vapor plasma yielded H₂O₂ concentrations of ≈0.8, 0.7 and 0.6 mM, respectively, and the pure N₂ plasma produced only 0.3 mM of H₂O₂. Among the different HNO₃ vapor plasmas, the 0.5 wt% of HNO₃ plasma generated the highest H₂O₂ concentration.

For NO, we found the opposite results as for the OH radicals and H₂O₂, i.e., a higher amount of NO was observed for N₂ + (0.5, 1, and 3 wt%) HNO₃ vapor plasma, as compared to the pure N₂ plasma and the N₂ + H₂O vapor plasma, as shown in Fig. 4(c). This is logical, because the HNO₃ vapor generates more NO upon dissociation, both in gas and liquid phase. For the same reason, NO₂⁻ and NO₃⁻ showed similar results: the N₂ + HNO₃ vapor plasma (at different wt%) yields higher NO₂⁻ and NO₃⁻ concentrations, as compared to the pure N₂ plasma

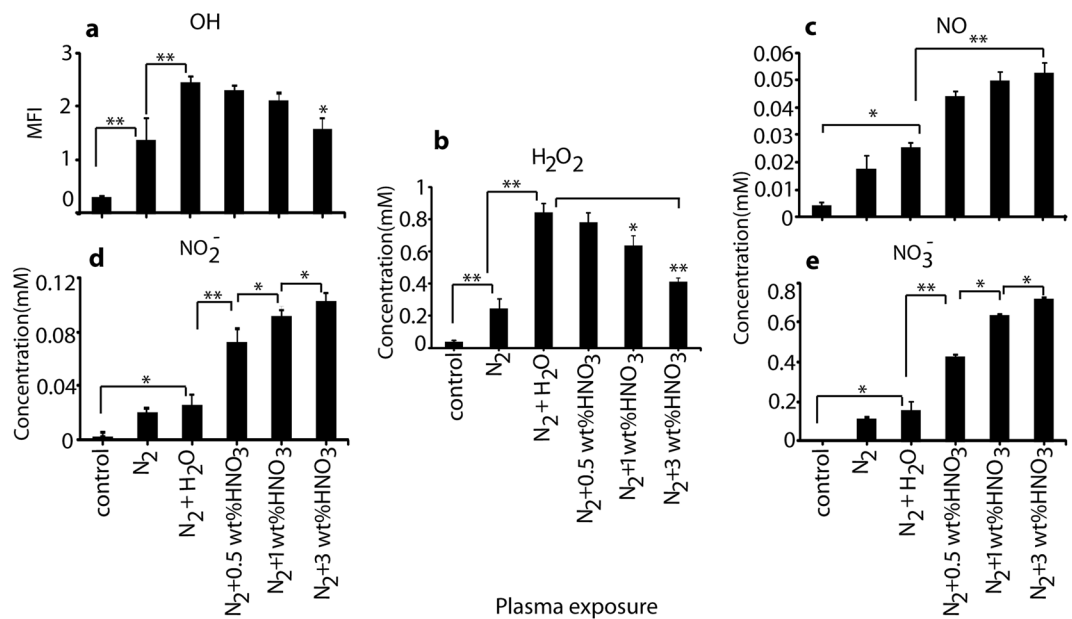


Figure 4. Determination of (a) hydroxyl radical; (b) hydrogen peroxide; (c) nitric oxide; (d) nitrite and (e) nitrate in DI water after exposure with plasma jet for 10 min, at different conditions (see Fig. 3).

and the $N_2 + H_2O$ vapor plasma, as shown in Fig. 4(d,e). The 3 wt% HNO_3 vapor system produced the highest amounts of NO, NO_2^- and NO_3^- .

Although 3 and 1 wt% HNO_3 vapor produces more RNS in comparison to 0.5 wt% HNO_3 vapor, the exposed water at these conditions becomes much more acidic, as shown in Fig. 3a. Hence, to avoid the effect of pH in bacterial inactivation, we have chosen the $N_2 + 0.5$ wt% HNO_3 vapor plasma system for the further research.

Efficacy of PTW generated with N_2 , $N_2 + H_2O$ vapor and $N_2 + 0.5$ wt% HNO_3 vapor plasma in *E. coli* inactivation, and comparison with direct plasma treatment.

To determine the efficacy of PTW produced by N_2 , $N_2 + H_2O$ vapor, and $N_2 + 0.5$ wt% HNO_3 vapor plasma, we checked the *E. coli* inactivation after 3 h incubation. Figure 5(a,b) show that exposure with PTW generated in case of 0.5 wt% HNO_3 vapor has a higher effect on *E. coli* inactivation, as its CFU reduces by 5 log values. The pure N_2 generated PTW reduces the CFU by 2 log values, while the PTW generated by $N_2 + H_2O$ vapor reduces the CFU by 4 log values. In comparison, PTW exposed to N_2 , $N_2 + H_2O$ vapor, and $N_2 + 0.5$ wt% HNO_3 vapor gas flow (i.e., without plasma) has no effect on *E. coli* inactivation (Fig. 5(c)), which indicates that the effects are clearly due to the RONS created by the plasma. Figure 5(d,e) show similar results in the disc diffusion assay: PTW created by $N_2 + 0.5$ wt% HNO_3 vapor has a higher zone of inhibition, in comparison with N_2 PTW and $N_2 + H_2O$ PTW.

To confirm this result, we also used the standard antibiotics agent (Penicillin) to check the zone of inhibition, and the results reveal that PTW created by $N_2 + 0.5$ wt% HNO_3 vapor has strong ability for zone of inhibition similar to Penicillin but higher as compare to $N_2 + H_2O$ PTW. Furthermore, we checked the effect of direct plasma action on *E. coli*. Figure S1 shows that direct treatment by $N_2 + 0.5$ wt% HNO_3 vapor plasma leads to significant inactivation of *E. coli*, in comparison with N_2 plasma and $N_2 + H_2O$ vapor plasma treatments. Hence, both direct and PTW treatment using $N_2 + 0.5$ wt% HNO_3 vapor plasma results in the maximum inactivation of *E. coli*.

Analysis of oxidative stress related gene expression and disruption of *E. coli* cell morphology.

To elucidate the mechanism of action of PTW on *E. coli* inactivation, we analyzed the oxidative related gene expression and cell morphology. For the gene expression analysis, we chose four oxidative stress genes, i.e., OxyR (Oxygen regulated gene), RpoE (DNA-dependent RNA polymerase), GroES (Heat-shock gene), and DnaK (Chaperone protein DnaK). These proteins regulate under stress conditions, and help to protect the cells through antioxidant defense mechanisms^{35–38}. OxyR and DnaK genes relates to oxidative stress. GroES and DnaK genes relates to the cellular homeostasis^{39,40}. The failure of the antioxidant defense machinery under high oxidative stress may lead to inhibitory effects of these gene expressions (OxyR, DnaK, GroES and DnaK) that results in DNA damage. Figure 6(a) shows that 3 h incubation of PTW generated by $N_2 + H_2O$ vapor or 0.5 wt% HNO_3 vapor caused higher inhibitions of the gene expression as compared with N_2 generated PTW. In contrast, PTW generated by $N_2 + H_2O$ or 0.5 wt% HNO_3 vapor shows inhibition of these gene expressions, because the oxidative stress is above the threshold under these PTW treatments, resulting in collapse of the antioxidant defense machinery.

We also determined the effects of PTW on the morphology of *E. coli*. Figure 6(b) shows that PTW generated by $N_2 + H_2O$ vapor and by $N_2 + 0.5$ wt% HNO_3 vapor has crumpled the cells to a greater extent than N_2 PTW. Finally, we checked the genomic DNA damage through 1% gel electrophoresis. Figures 6(c) and S2 shows that

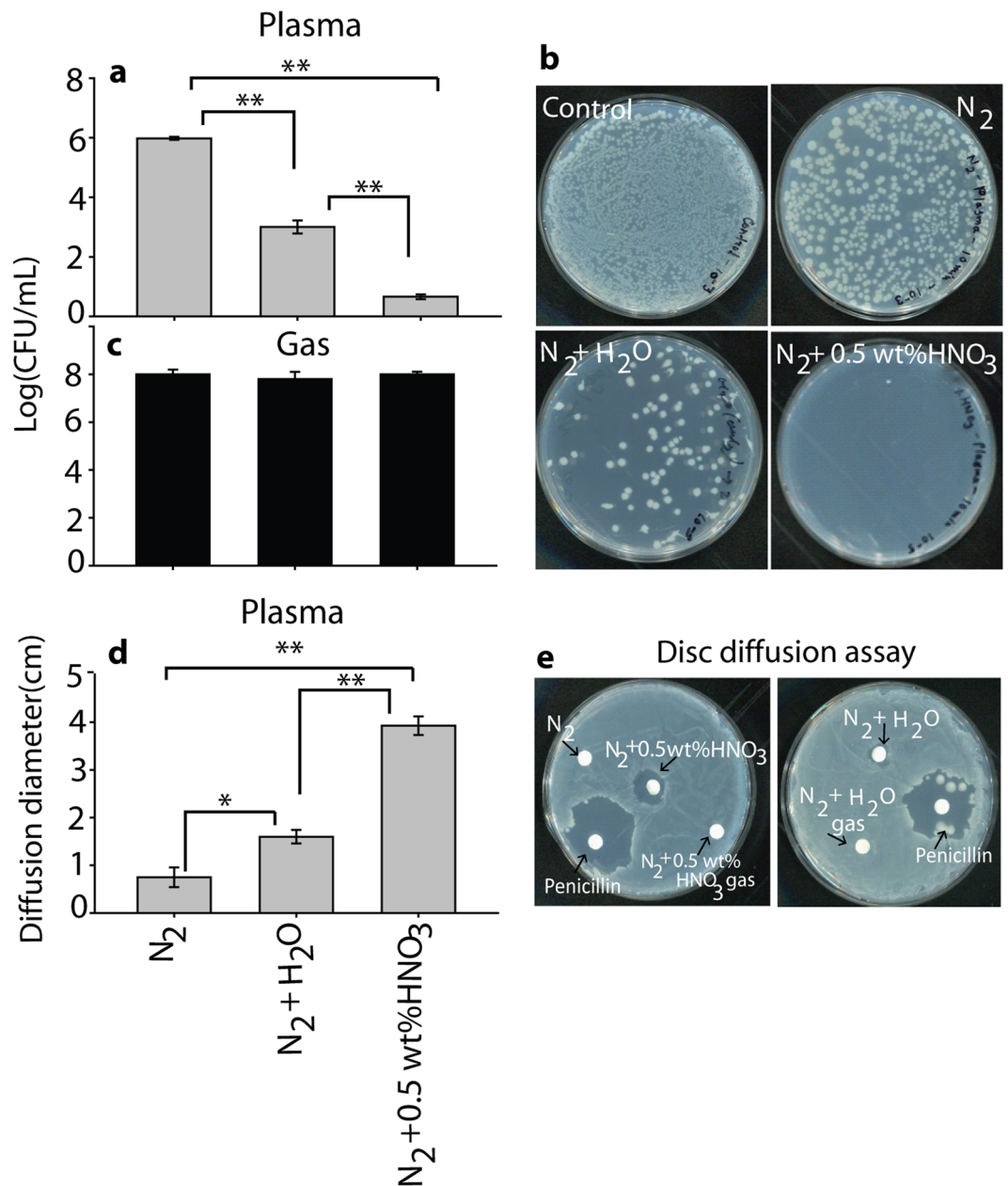


Figure 5. (a) Inactivation of *E. coli* after different types of PTW treatments, (b) Colony of *E. coli* inactivation after different types of PTW treatments, (c) Inactivation of *E. coli* after gas treated water and (d,e) Disc diffusion assay after 3 hr incubation with PTW generated by N₂, N₂ + H₂O vapor and N₂ + 0.5% HNO₃ vapor.

PTW generated by N₂ + H₂O vapor and N₂ + 0.5 wt% HNO₃ vapor have more effect on the DNA degradation/oxidation.

Discussions

It is generally known that RONS generated from an APPJ induce inactivation of microorganisms, as well as structural changes in proteins^{5,32}. In this work, we demonstrate that the adding a vapor system (either water vapor or 0.5 wt% of HNO₃ vapor) to the plasma enhances the antimicrobial activity as compared to plasma without vapor system. This is attributed to the increase in ROS and RNS content. The H₂O vapor system increases the ROS in the solution, but the RNS formation does not increase, whereas the HNO₃ vapor system can increase both the RNS and ROS content in solution. We analyzed the NO and OH species by optical emission spectrometry in the gas phase and by chemical analysis in the solution, after 10 min plasma treatment. The NO radical concentration dramatically increases inside the solution for plasma treatment with N₂ (400 ccm) + 0.5 wt% HNO₃ vapor (600 ccm N₂ gas), as compared to pure N₂ plasma treatment or treatment by N₂ + H₂O vapor. At this condition, both the NO and OH concentrations increase in the gas phase, as well as inside the solution. On the other hand, for

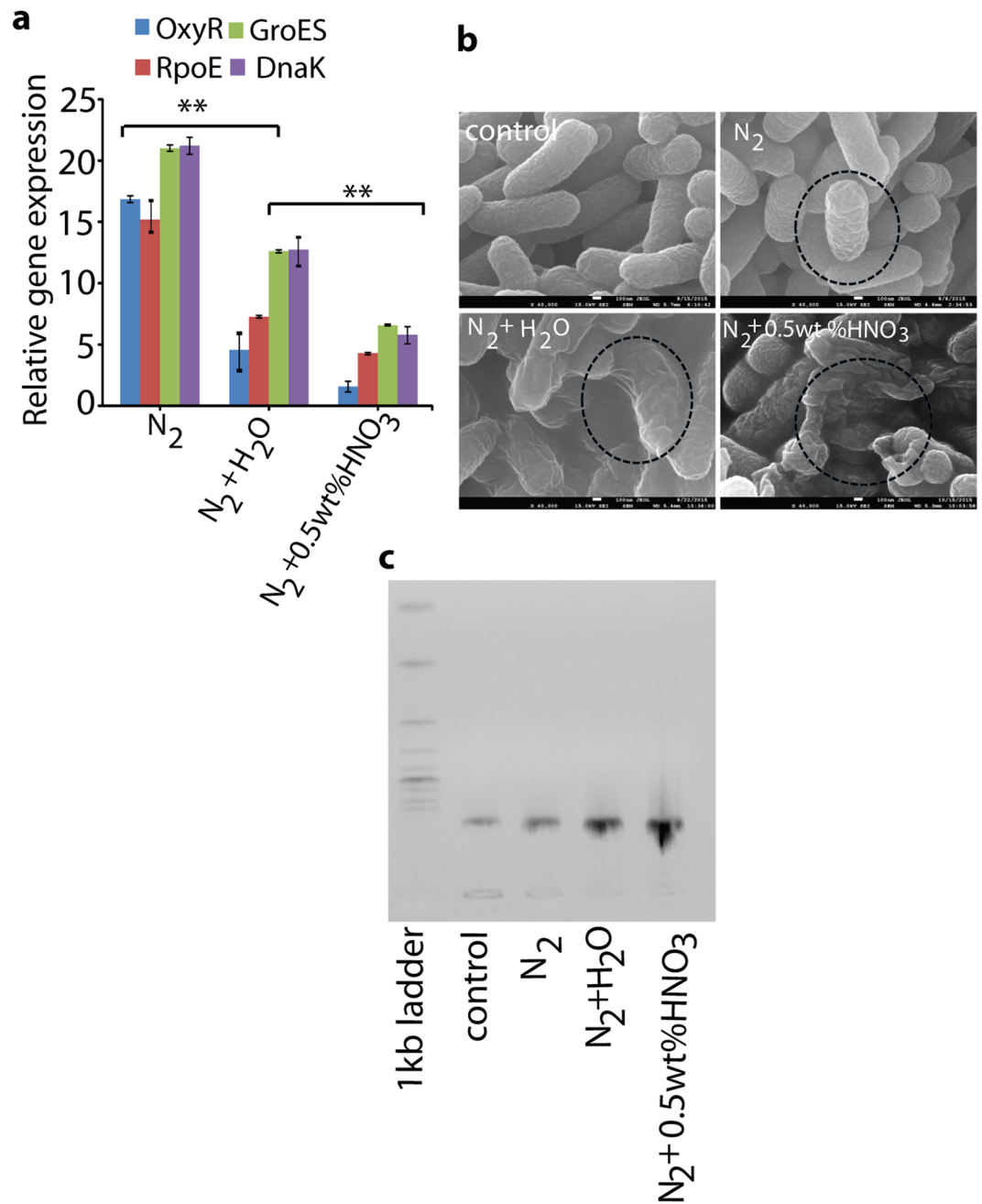


Figure 6. (a) Analysis of oxidative related gene expressions, (b) cell morphology and (c) DNA damage after 3 hr incubation with PTW generated by N_2 , $N_2 + H_2O$ vapor and $N_2 + 0.5\% HNO_3$ vapor.

the water vapor system, the OH content increases by a large amount, but the NO concentration did not increase in solution, as shown in Fig. 4.

We measured the transcriptional level of these genes (OxyR, RpoE, GroES, and DnaK) in PTW-treated *E. coli*. When *E. coli* was treated with N_2 PTW, the transcriptional-related gene expressions of OxyR, RpoE, GroES, and DnaK were enhanced (Fig. 6(a)). In contrast, the $N_2 + H_2O$ or 0.5 wt% HNO_3 PTW showed inhibitory effects on the gene expression in comparison with the control sample. Furthermore, $N_2 + 0.5\% HNO_3$ PTW showed higher inhibition effect than $N_2 + H_2O$ PTW, which can be explained by the higher RONS content. This study clearly shows that PTW generated by $N_2 + H_2O$ vapor or 0.5 wt% HNO_3 vapor plasma has higher RONS contents, which lead to bacteria killing through inhibition of the antioxidant machinery, which damages the membrane protein repair chaperone, as well as DNA repair cascade^{41,42}. Furthermore, we analyzed the DNA degradation through gel electrophoresis and the bacteria morphology, after treatment with PTW generated by all plasma systems. Among all systems (N_2 plasma, $N_2 + H_2O$ vapor plasma, and $N_2 + 0.5\% HNO_3$ vapor plasma), the PTW generated by $N_2 + 0.5\% HNO_3$ vapor plasma shows more *E. coli* deactivation.

This study demonstrates that PTW produced from $N_2 + H_2O$ vapor plasma and $N_2 + 0.5 \text{ wt\% } HNO_3$ vapor plasma systems has a high antibacterial efficiency. According to literature, NO_2^- and H_2O_2 are important for the bactericidal activity²¹. At our experimental conditions, the N_2 plasma produces $\approx 0.02 \text{ mM } NO_2^-$ and $\approx 0.3 \text{ mM } H_2O_2$, while the $N_2 + H_2O$ vapor plasma produces $\approx 0.025 \text{ mM } NO_2^-$ and $\approx 0.9 \text{ mM } H_2O_2$, and the $N_2 + 0.5 \text{ wt\% } HNO_3$ vapor plasma produces ≈ 0.076 and 0.8 mM of NO_2^- and H_2O_2 , respectively. Thus, the maximum NO_2^- and H_2O_2 concentrations are produced by the $N_2 + 0.5 \text{ wt\% } HNO_3$ vapor plasma and the $N_2 + H_2O$ vapor plasma, respectively. If we compare the bactericidal activity in Fig. 5, we observe the maximum deactivation of bacteria for the PTW generated by the $N_2 + 0.5 \text{ wt\% } HNO_3$ vapor plasma, followed by the $N_2 + H_2O$ vapor plasma, and the smallest effect for the N_2 plasma PTW. This shows that a high concentration of both NO_2^- and H_2O_2 plays a key role in sterilization. It was reported previously that the presence of H_2O_2 and HNO_2 produces $ONOO^-$, which is the main component for inactivation of bacteria²⁸. However, $ONOO^-$ has a short lifetime in acidic solution, and therefore it cannot be the main component of PTW for the antibacterial activity^{26,30}. On the other hand, Ikawa *et al.* reported that $O_2^{\bullet-}$ is mainly responsible for the bactericidal activity³¹. The authors also claimed that the production of $O_2^{\bullet-}$ does not require the presence of oxygen, as it is generated by O_2NOOH . They also suggested that H_2O_2 is the main component for the production of O_2NOOH in PTW along with NO_2^- . Therefore, we may conclude that the $N_2 + 0.5 \text{ wt\% } HNO_3$ vapor plasma produces the highest amount of NO_2^- and H_2O_2 in PTW, which can form O_2NOOH by multiple reactions, and this further leads to the formation of $O_2^{\bullet-}$ which contributes to sterilization. On the other hand, the $N_2 + H_2O$ vapor plasma produces a high amount of H_2O_2 but a lower content of NO_2^- ; and this results in a lower production of $O_2^{\bullet-}$, and thus in a lower antibacterial activity. Additionally, the pH of PTW after $N_2 + 0.5 \text{ wt\% } HNO_3$ vapor plasma and $N_2 + H_2O$ vapor plasma is near 4.5, and it was reported that the half-life of O_2NOOH is 1.6 min at pH 4.7⁴³. Hence, we believe that in our study O_2NOOH is the main factor for the bactericidal activity through $O_2^{\bullet-}$ formation.

Conclusion

We studied the antibacterial effect of PTW generated by various plasma systems, i.e., N_2 plasma, $N_2 + H_2O$ vapor plasma, and $N_2 + 0.5 \text{ wt\% } HNO_3$ vapor plasma, and we clearly demonstrated that the vapor plasma, and especially the $N_2 + 0.5 \text{ wt\% } HNO_3$ vapor plasma, was more efficient for the deactivation of bacteria than PTW generated by plasma without vapor system. The results of this research support the idea that a high concentration of both NO_2^- and H_2O_2 is important for the antibacterial activity, through the creation of other RONS, such as O_2NOOH and $O_2^{\bullet-}$.

References

- Moreau, M. *et al.* Non-thermal plasma technologies: New tools for bio-decontamination. *Biotechnol Adv.* **26**, 610–617 (2008).
- Cheng, H. H. *et al.* Non-thermal plasma technology for degradation of organic compounds in wastewater control: A critical review. *J. Environ. Eng. Manage* **17**, 427–433 (2007).
- Attri, P. *et al.* Impact of Gamma rays and DBD plasma treatments on wastewater treatment. *Sci Rep.* **8**, 2926 (2018).
- Ehlbeck, J. *et al.* Low temperature atmospheric pressure plasma sources for microbial decontamination. *J. Phys. D: Appl. Phys.* **44**, 013002 (2010).
- Park, J. H. *et al.* A comparative study for the inactivation of multidrug resistance bacteria using dielectric barrier discharge and nano-second pulsed plasma. *Sci Rep.* **5**, 13849 (2015).
- Attri, P. *et al.* Influence of reactive species on the modification of biomolecules generated from the soft plasma. *Sci Rep.* **5**, 8221 (2015).
- Laroussi, M. Low temperature plasma-based sterilization: overview and state-of-the-art. *Plasma Process. Polym.* **2**, 391–400 (2005).
- Xu, G. M. *et al.* Dual effects of atmospheric pressure plasma jet on skin wound healing of mice. *Wound Repair Regen.* **23**, 878–884 (2015).
- Bekeschus, S. *et al.* Human mononuclear cell survival and proliferation is modulated by cold atmospheric plasma jet. *Plasma Process. Polym.* **10**, 706–713 (2013).
- Wende, K. *et al.* Atmospheric pressure plasma jet treatment evokes transient oxidative stress in HaCaT keratinocytes and influences cell physiology. *Cell Biol Int.* **38**, 412–425 (2014).
- Fathollah, S. *et al.* Investigation on the effects of the atmospheric pressure plasma on wound healing in diabetic rats. *Sci Rep.* **6**, 19144 (2016).
- Lee, J.-H. *et al.* Effect of non-thermal air atmospheric pressure plasma jet treatment on gingival wound healing. *J. Phys. D: Appl. Phys.* **49**, 075402 (2016).
- Kumar, N. *et al.* Influence of Nitric Oxide generated through microwave plasma on L6 skeletal muscle cell myogenesis via oxidative signaling pathways. *Sci Rep.* **7**, 542 (2017).
- Kumar, N. *et al.* Induced apoptosis in melanocytes cancer cell and oxidation in biomolecules through deuterium oxide generated from atmospheric pressure non-thermal plasma jet. *Sci Rep.* **4**, 7589 (2014).
- Van Boxem, W. *et al.* Anti-cancer capacity of plasma-treated PBS: effect of chemical composition on cancer cell cytotoxicity. *Sci Rep.* **7**, 16478 (2017).
- Kumar, N. *et al.* Influence of water vapour with non-thermal plasma jet on the apoptosis of SK-BR-3 breast cancer cells. *RSC Adv.* **5**, 14670–14677 (2015).
- Mohades, S. *et al.* Evaluation of the effects of a plasma activated medium on cancer cells. *Phys. Plasmas.* **22**, 122001 (2015).
- Boehm, D. *et al.* Cytotoxic and mutagenic potential of solutions exposed to cold atmospheric plasma. *Sci Rep.* **6**, 21464 (2016).
- Kumar, N. *et al.* The action of microsecond-pulsed plasma-activated media on the inactivation of human lung cancer cells. *J. Phys. D: Appl. Phys.* **49**, 115401 (2016).
- Adachi, T. *et al.* Plasma-activated medium induces A549 cell injury via a spiral apoptotic cascade involving the mitochondrial–nuclear network. *Free Radic Biol Med.* **79**, 28–44 (2015).
- Shen, J. *et al.* Bactericidal Effects against *S. aureus* and Physicochemical Properties of Plasma Activated Water stored at different temperatures. *Sci Rep.* **6**, 28505 (2016).
- Reuter, S. *et al.* Generation of atomic oxygen in the effluent of an APPJ. *Plasma Sources Sci. Technol.* **18**, 015006 (2009).
- Glaze, W. H. *et al.* The Chemistry of water treatment processes involving ozone, hydrogen peroxide and ultraviolet radiation. *Ozone Sci. Eng.* **9**, 335–352 (1987).
- Sun, P. *et al.* Inactivation of *Bacillus subtilis* Spores in Water by a Direct-Current, Cold Atmospheric-Pressure Air Plasma Microjet. *Plasma Process. Polym.* **9**, 157–164 (2012).
- Traylor, M. J. *et al.* Long-term antibacterial efficacy of air plasma-activated water. *J. Phys. D: Appl. Phys.* **44**, 472001 (2011).

26. Zhang, Q. *et al.* A study of oxidative stress induced by non-thermal plasma-activated water for bacterial damage. *Appl. Phys. Lett.* **102**, 203701 (2013).
27. Machala, Z. *et al.* Formation of ROS and RNS in water electro-sprayed through transient spark discharge in air and their bactericidal effects. *Plasma Process. Polym.* **10**, 649–659 (2013).
28. Lukes, P. *et al.* Aqueous-phase chemistry and bactericidal effects from an air discharge plasma in contact with water: evidence for the formation of peroxyxynitrite through a pseudo-second-order post-discharge reaction of H₂O₂ and HNO₂. *Plasma Sources Sci. Technol.* **23**, 015019 (2014).
29. Oehmigen, K. *et al.* Estimation of possible mechanisms of *Escherichia coli* inactivation by plasma treated sodium chloride solution. *Plasma Process. Polym.* **8**, 904–913 (2011).
30. Naïtali, M. *et al.* Combined effects of long-living chemical species during microbial inactivation using atmospheric plasma-treated water. *Appl. Environ. Microbiol.* **76**, 7662–7664 (2010).
31. Ikawa, S. *et al.* Physicochemical properties of bactericidal plasma-treated water. *J. Phys. D: Appl. Phys.* **49**, 425401 (2016).
32. Attri, P. *et al.* The protective action of osmolytes on the deleterious effects of gamma rays and atmospheric pressure plasma on protein conformational changes. *Sci Rep.* **7**, 8698 (2017).
33. Park, J. H. *et al.* Variation in structure of proteins by adjusting reactive oxygen and nitrogen species generated from dielectric barrier discharge jet. *Sci Rep.* **6**, 35883 (2016).
34. Bauer, A. *et al.* Antibiotic susceptibility testing by a standardized single disk method. *Am J Clin Pathol.* **45**, 493 (1966).
35. Kilstrup, M. *et al.* Induction of Heat Shock Proteins DnaK, GroEL, and GroES by Salt Stress in *Lactococcus lactis*. *Appl. Environ. Microbiol.* **63**, 1826–1837 (1997).
36. Wang, A. & Crowley, D. E. Global Gene Expression Responses to Cadmium Toxicity in *Escherichia coli*. *J. Bacteriol.* **187**, 3259–3266 (2005).
37. Mongkolsuk, S. & Helmann, J. D. Regulation of inducible peroxide stress responses. *Mol. Microbiol.* **45**, 9–15 (2002).
38. Hiratsu, K. *et al.* The rpoE Gene of *Escherichia coli*, Which Encodes sigma E, Is Essential for Bacterial Growth at High Temperature. *J. Bacteriol.* **177**, 2918–2922 (1995).
39. Houry, W. A. Chaperone-assisted protein folding in the cell cytoplasm. *Curr. Protein Pept. Sci.* **2**, 227–244 (2001).
40. Lin, Z. & Rye, H. S. GroEL-mediated protein folding: making the impossible, possible. *Crit. Rev. Biochem. Mol. Biol.* **41**, 211–239 (2006).
41. Vatansever, F. *et al.* Antimicrobial strategies centered around reactive oxygen species–bactericidal antibiotics, photodynamic therapy, and beyond. *FEMS Microbiol. Rev.* **37**, 955–989 (2013).
42. Pomposiello, P. & Demple, B. Global adjustment of microbial physiology during free radical stress. *Adv. Microb. Physiol.* **46**, 19–341 (2002).
43. Kenley, R. A., Trevor, P. L. & Lan, B. Y. Preparation and thermal decomposition of pernitric acid (HOONO₂) in aqueous media. *J. Amer. Chem. Soc.* **103**, 2203–2206 (1981).

Acknowledgements

We gratefully acknowledge the Leading Foreign Research Institute Recruitment program (Grant # NRF-2016K1A4A3914113) throughout the Basic Science Research Program of the National Research Foundation (NRF) of Korea and in part by Kwangwoon University 2018. JHP thanks to NRF Grant No. NRF-2017R1D1A1B03033495. We also acknowledge financial support from the Research Foundation – Flanders (FWO) (Grant Number 12J5617N) and from the European Marie Skłodowska-Curie Individual Fellowship “Anticancer-PAM” within Horizon 2020 (Grant Number 743546).

Author Contributions

P.A. designed the experiments and conceived the manuscript. P.A. and A.B. wrote the manuscript. N.K. and P.A. analyzed the data. P.S., N.K., H.S.K., and J.H.P. performed the research. A.B., H.S.U. and E.H.C. supervised the project. H.S.U. and P.A. designed the plasma setup.

Additional Information

Supplementary information accompanies this paper at <https://doi.org/10.1038/s41598-018-29549-6>.

Competing Interests: The authors declare no competing interests.

Publisher's note: Springer Nature remains neutral with regard to jurisdictional claims in published maps and institutional affiliations.



Open Access This article is licensed under a Creative Commons Attribution 4.0 International License, which permits use, sharing, adaptation, distribution and reproduction in any medium or format, as long as you give appropriate credit to the original author(s) and the source, provide a link to the Creative Commons license, and indicate if changes were made. The images or other third party material in this article are included in the article's Creative Commons license, unless indicated otherwise in a credit line to the material. If material is not included in the article's Creative Commons license and your intended use is not permitted by statutory regulation or exceeds the permitted use, you will need to obtain permission directly from the copyright holder. To view a copy of this license, visit <http://creativecommons.org/licenses/by/4.0/>.

© The Author(s) 2018